

Exclusive $pp \rightarrow nn\pi^+\pi^+$ reaction at LHC and RHIC

P. Lebiedowicz^{1,*} and A. Szczurek^{2,1,†}

¹*Institute of Nuclear Physics PAN, PL-31-342 Cracow, Poland*

²*University of Rzeszów, PL-35-959 Rzeszów, Poland*

Abstract

We evaluate differential distributions for the four-body $pp \rightarrow nn\pi^+\pi^+$ reaction. The amplitude for the process is calculated in the Regge approach including many diagrams. We make predictions for possible future experiments at RHIC and LHC energies. Very large cross sections are found which is partially due to interference of a few mechanisms. Absorption effects are estimated. Differential distributions in pseudorapidity, rapidity, invariant two-pion mass, transverse-momentum and energy distributions of neutrons are presented for proton-proton collisions at $\sqrt{s} = 200, 500$ GeV (RHIC) and $\sqrt{s} = 0.9, 2.36$ and 7 TeV (LHC). Cross sections with experimental cuts are presented.

PACS numbers: 11.55.Jy, 13.85.Lg, 14.20.Dh

*Electronic address: piotr.lebiedowicz@ifj.edu.pl

†Electronic address: antoni.szczurek@ifj.edu.pl

I. INTRODUCTION

It was realized over the last decade that the measurement of forward particles can be an interesting and useful supplement to the central multipurpose LHC detectors (ATLAS, CMS). The main effort concentrated on the design and construction of forward proton detectors [1]. Also Zero-Degree Calorimeters (ZDC's) have been considered as a useful supplement. It will measure very forward neutrons and photons in the pseudorapidity region $|\eta| \geq 8.5$ at the CMS [2] (see also [3]) and the ATLAS ZDC's provide coverage of the region $|\eta| \geq 8.3$ [4]. It was shown recently that the CMS (Compact Muon Spectrometer) Collaboration ZDC's provide a unique possibility to measure the $\pi^+\pi^+$ total cross section [5].

In the present paper we consider an example of an exclusive reaction with two forward neutrons. Given the experimental infrastructure the $pp \rightarrow nn\pi^+\pi^+$ is one of the reactions with four particles in the final state which could be addressed at LHC. The diagrams of the process (with four-momenta $p_a + p_b \rightarrow p_1 + p_2 + p_3 + p_4$) are presented in Fig.1.

In the present analysis we will also include absorption effects as was done recently for three-body processes [6].

II. THE AMPLITUDE

A. Bare diffractive amplitude

The diffractive mechanisms involving pomeron and reggeon exchanges included in the present paper are shown in Fig.1. The diagrams will be called a) – j) for brevity. In the present analysis we consider diagrams with pomeron (P) and reggeon exchanges. In diagrams a) – i) both pomeron and reggeon exchanges are possible while in diagram j) only ρ reggeon is possible. For simplicity we use linear trajectory of the pomeron and reggeons, but further improvements are possible.

In principle in all diagrams shown the intermediate nucleon can be replaced by nucleon excited states. The contribution of such diagrams is however much smaller. First of all the diffractive transitions are known to be much weaker than the elastic one. Secondly the $g_{NN^*\pi}$ coupling constants are much smaller than the $g_{NN\pi}$ coupling constant [7]. Finally the exact strength of the diffractive transitions are not known phenomenologically. Therefore in the following we neglect the contributions of diagrams with excited nucleon states.

In addition to diagram (j) there is possible also another mechanism with the intermediate pion replaced by a virtual photon. Because it requires two electromagnetic couplings instead of two strong couplings its contribution should be small. Because of the extra photon propagator it could be enhanced when $k_\gamma^2 \rightarrow 0$. However then the vertices should tend to zero. Therefore we can safely omit such a diagram.

Similarly as for the $p\bar{p} \rightarrow N\bar{N}f_0(1500)$ [8] and $pp \rightarrow pp\pi^+\pi^-$ ($p\bar{p} \rightarrow p\bar{p}\pi^+\pi^-$) [9, 10] reactions the amplitudes can be written in terms of pomeron (reggeon)-exchanges. Then the amplitude squared, averaged over the initial and summed over the final polarization states, for the $pp \rightarrow nn\pi^+\pi^+$ process can be written as:

$$\overline{|\mathcal{M}|^2} = \frac{1}{4} \sum_{\lambda_a \lambda_b \lambda_1 \lambda_2} |\mathcal{M}_{\lambda_a \lambda_b \rightarrow \lambda_1 \lambda_2}^{(a)} + \dots + \mathcal{M}_{\lambda_a \lambda_b \rightarrow \lambda_1 \lambda_2}^{(i)}|^2. \quad (2.1)$$

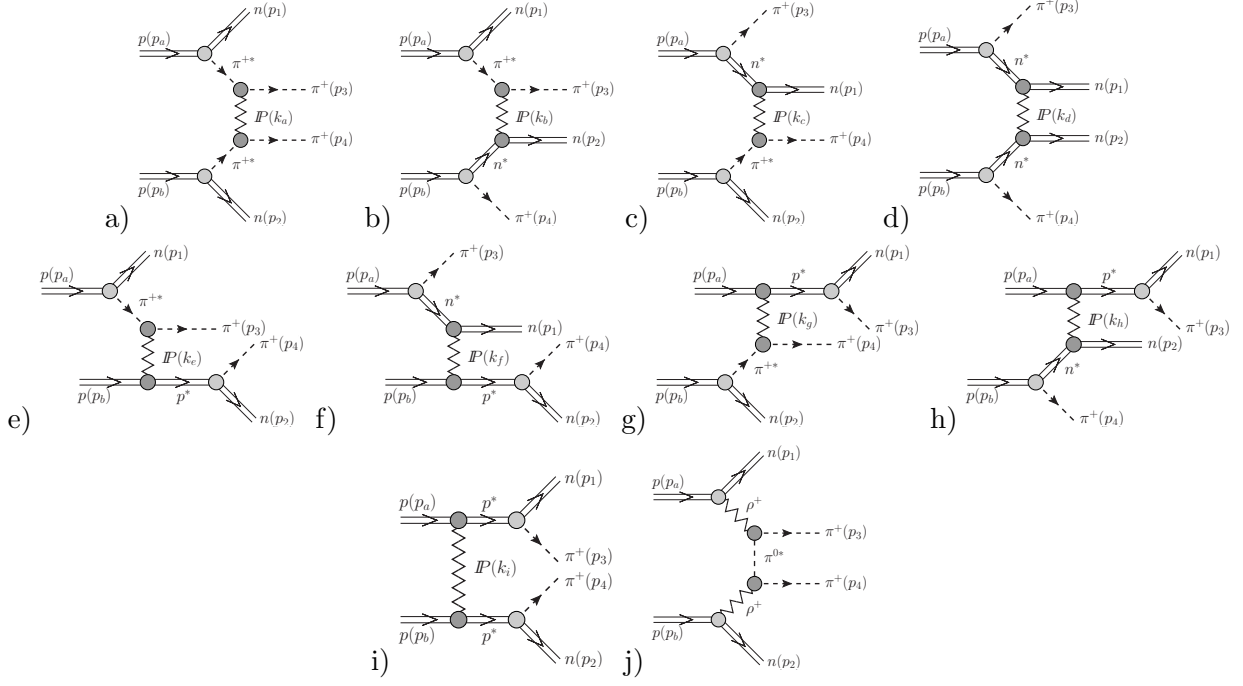


FIG. 1: Diagrams for the exclusive production of $\pi^+\pi^+$ in pp collisions at high energies. The stars attached to π^+ , n and p denote the fact they are off-mass-shell. k_a-k_i are four-vectors of the exchanged pomerons.

It is straightforward to evaluate the contribution shown in Fig.1. If we assume the $i\gamma_5$ type coupling of the pion to the nucleon then the Born amplitudes read: ¹

$$\begin{aligned}
\mathcal{M}_{\lambda_a \lambda_b \rightarrow \lambda_1 \lambda_2}^{(a)} = & \bar{u}(p_1, \lambda_1) i\gamma_5 S_\pi(t_1) u(p_a, \lambda_a) \sqrt{2} g_{\pi NN} F_{\pi NN}(t_1) \\
& \times F_\pi^{off}(t_1) i s_{34} C_P^{\pi\pi} \left(\frac{s_{34}}{s_0} \right)^{\alpha_P(k_a^2)-1} \exp\left(\frac{B_{\pi\pi}}{2} k_a^2\right) F_\pi^{off}(t_2) \\
& \times \bar{u}(p_2, \lambda_2) i\gamma_5 S_\pi(t_2) u(p_b, \lambda_b) \sqrt{2} g_{\pi NN} F_{\pi NN}(t_2), \quad (2.2)
\end{aligned}$$

$$\begin{aligned}
\mathcal{M}_{\lambda_a \lambda_b \rightarrow \lambda_1 \lambda_2}^{(b)} = & \bar{u}(p_1, \lambda_1) i\gamma_5 S_\pi(t_1) u(p_a, \lambda_a) \sqrt{2} g_{\pi NN} F_{\pi NN}(t_1) \\
& \times F_\pi^{off}(t_1) i s_{23} C_P^{\pi N} \left(\frac{s_{23}}{s_0} \right)^{\alpha_P(k_b^2)-1} \exp\left(\frac{B_{\pi N}}{2} k_b^2\right) F_n^{off}(u_2) \\
& \times \bar{u}(p_2, \lambda_2) i\gamma_5 S_n(u_2) u(p_b, \lambda_b) \sqrt{2} g_{\pi NN} F_{\pi NN}(u_2), \quad (2.3)
\end{aligned}$$

$$\begin{aligned}
\mathcal{M}_{\lambda_a \lambda_b \rightarrow \lambda_1 \lambda_2}^{(c)} = & \bar{u}(p_1, \lambda_1) i\gamma_5 S_n(u_1) u(p_a, \lambda_a) \sqrt{2} g_{\pi NN} F_{\pi NN}(u_1) \\
& \times F_n^{off}(u_1) i s_{14} C_P^{\pi N} \left(\frac{s_{14}}{s_0} \right)^{\alpha_P(k_c^2)-1} \exp\left(\frac{B_{\pi N}}{2} k_c^2\right) F_\pi^{off}(t_2) \\
& \times \bar{u}(p_2, \lambda_2) i\gamma_5 S_\pi(t_2) u(p_b, \lambda_b) \sqrt{2} g_{\pi NN} F_{\pi NN}(t_2), \quad (2.4)
\end{aligned}$$

¹ We show explicitly only amplitudes for pomeron exchange. The amplitudes for reggeon exchange can be obtained from those for pomeron exchange by replacing propagators, signature factors and trajectories.

$$\begin{aligned}
\mathcal{M}_{\lambda_a \lambda_b \rightarrow \lambda_1 \lambda_2}^{(d)} = & \bar{u}(p_1, \lambda_1) i\gamma_5 S_n(u_1) u(p_a, \lambda_a) \sqrt{2} g_{\pi NN} F_{\pi NN}(u_1) \\
& \times F_n^{off}(u_1) i s_{12} C_{\mathbb{P}}^{NN} \left(\frac{s_{12}}{s_0} \right)^{\alpha_{\mathbb{P}}(k_d^2)-1} \exp \left(\frac{B_{NN}}{2} k_d^2 \right) F_n^{off}(u_2) \\
& \times \bar{u}(p_2, \lambda_2) i\gamma_5 S_n(u_2) u(p_b, \lambda_b) \sqrt{2} g_{\pi NN} F_{\pi NN}(u_2) , \tag{2.5}
\end{aligned}$$

$$\begin{aligned}
\mathcal{M}_{\lambda_a \lambda_b \rightarrow \lambda_1 \lambda_2}^{(e)} = & \bar{u}(p_1, \lambda_1) i\gamma_5 S_\pi(t_1) u(p_a, \lambda_a) \sqrt{2} g_{\pi NN} F_{\pi NN}(t_1) \\
& \times F_\pi^{off}(t_1) i s_{234} C_{\mathbb{P}}^{\pi N} \left(\frac{s_{234}}{s_0} \right)^{\alpha_{\mathbb{P}}(k_e^2)-1} \exp \left(\frac{B_{\pi N}}{2} k_e^2 \right) F_p^{off}(s_{24}) \\
& \times \bar{u}(p_2, \lambda_2) i\gamma_5 S_p(s_{24}) u(p_b, \lambda_b) \sqrt{2} g_{\pi NN} F_{\pi NN}(s_{24}) , \tag{2.6}
\end{aligned}$$

$$\begin{aligned}
\mathcal{M}_{\lambda_a \lambda_b \rightarrow \lambda_1 \lambda_2}^{(f)} = & \bar{u}(p_1, \lambda_1) i\gamma_5 S_n(u_1) u(p_a, \lambda_a) \sqrt{2} g_{\pi NN} F_{\pi NN}(u_1) \\
& \times F_n^{off}(u_1) i s_{124} C_{\mathbb{P}}^{NN} \left(\frac{s_{124}}{s_0} \right)^{\alpha_{\mathbb{P}}(k_f^2)-1} \exp \left(\frac{B_{NN}}{2} k_f^2 \right) F_p^{off}(s_{24}) \\
& \times \bar{u}(p_2, \lambda_2) i\gamma_5 S_p(s_{24}) u(p_b, \lambda_b) \sqrt{2} g_{\pi NN} F_{\pi NN}(s_{24}) , \tag{2.7}
\end{aligned}$$

$$\begin{aligned}
\mathcal{M}_{\lambda_a \lambda_b \rightarrow \lambda_1 \lambda_2}^{(g)} = & \bar{u}(p_1, \lambda_1) i\gamma_5 S_p(s_{13}) u(p_a, \lambda_a) \sqrt{2} g_{\pi NN} F_{\pi NN}(s_{13}) \\
& \times F_p^{off}(s_{13}) i s_{134} C_{\mathbb{P}}^{\pi N} \left(\frac{s_{134}}{s_0} \right)^{\alpha_{\mathbb{P}}(k_g^2)-1} \exp \left(\frac{B_{\pi N}}{2} k_g^2 \right) F_\pi^{off}(t_2) \\
& \times \bar{u}(p_2, \lambda_2) i\gamma_5 S_\pi(t_2) u(p_b, \lambda_b) \sqrt{2} g_{\pi NN} F_{\pi NN}(t_2) , \tag{2.8}
\end{aligned}$$

$$\begin{aligned}
\mathcal{M}_{\lambda_a \lambda_b \rightarrow \lambda_1 \lambda_2}^{(h)} = & \bar{u}(p_1, \lambda_1) i\gamma_5 S_p(s_{13}) u(p_a, \lambda_a) \sqrt{2} g_{\pi NN} F_{\pi NN}(s_{13}) \\
& \times F_p^{off}(s_{13}) i s_{123} C_{\mathbb{P}}^{NN} \left(\frac{s_{123}}{s_0} \right)^{\alpha_{\mathbb{P}}(k_h^2)-1} \exp \left(\frac{B_{NN}}{2} k_h^2 \right) F_n^{off}(u_2) \\
& \times \bar{u}(p_2, \lambda_2) i\gamma_5 S_n(u_2) u(p_b, \lambda_b) \sqrt{2} g_{\pi NN} F_{\pi NN}(u_2) , \tag{2.9}
\end{aligned}$$

$$\begin{aligned}
\mathcal{M}_{\lambda_a \lambda_b \rightarrow \lambda_1 \lambda_2}^{(i)} = & \bar{u}(p_1, \lambda_1) i\gamma_5 S_p(s_{13}) u(p_a, \lambda_a) \sqrt{2} g_{\pi NN} F_{\pi NN}(s_{13}) \\
& \times F_p^{off}(s_{13}) i s_{ab} C_{\mathbb{P}}^{NN} \left(\frac{s_{ab}}{s_0} \right)^{\alpha_{\mathbb{P}}(k_i^2)-1} \exp \left(\frac{B_{NN}}{2} k_i^2 \right) F_p^{off}(s_{24}) \\
& \times \bar{u}(p_2, \lambda_2) i\gamma_5 S_p(s_{24}) u(p_b, \lambda_b) \sqrt{2} g_{\pi NN} F_{\pi NN}(s_{24}) , \tag{2.10}
\end{aligned}$$

$$\begin{aligned}
\mathcal{M}_{\lambda_a \lambda_b \rightarrow \lambda_1 \lambda_2}^{(j)} = & \sqrt{2} \delta_{\lambda_a, \lambda_1} (a_\rho - i) s_{13} C_\rho^{\pi N} \left(\frac{s_{13}}{s_0} \right)^{\alpha_\rho(t_1)-1} \exp \left(\frac{B_{\pi N}}{2} t_1 \right) \\
& \times F_\pi^{off}(k_\pi^2) \frac{1}{k_\pi^2 - m_\pi^2} F_\pi^{off}(k_\pi^2) \\
& \times \sqrt{2} \delta_{\lambda_b, \lambda_2} (a_\rho - i) s_{24} C_\rho^{\pi N} \left(\frac{s_{24}}{s_0} \right)^{\alpha_\rho(t_2)-1} \exp \left(\frac{B_{\pi N}}{2} t_2 \right) \\
& + \text{crossed term} . \tag{2.11}
\end{aligned}$$

In the above equations $u(p_i, \lambda_i)$, $\bar{u}(p_f, \lambda_f) = u^\dagger(p_f, \lambda_f) \gamma^0$ are the Dirac spinors (normalized as $\bar{u}(p)u(p) = 2m_N$) of the initial protons and outgoing neutrons with the four-momentum p and the helicities of the nucleons λ . The propagators of virtual particles can

be written as

$$S_\pi(t_{1,2}) = \frac{i}{t_{1,2} - m_\pi^2}, \quad (2.12)$$

$$S_n(u_{1,2}) = \frac{i(\tilde{u}_{1,2\nu}\gamma^\nu + m_n)}{u_{1,2} - m_n^2}, \quad (2.13)$$

$$S_p(s_{ij}) = \frac{i(\tilde{s}_{ij\nu}\gamma^\nu + m_p)}{s_{ij} - m_p^2}, \quad (2.14)$$

where $t_{1,2} = (p_{a,b} - p_{1,2})^2$ and $u_{1,2} = (p_{a,b} - p_{3,4})^2 = \tilde{u}_{1,2}^2$ are the four-momenta squared of transferred pions and neutrons², respectively. $s_{ij} = (p_i + p_j)^2 = \tilde{s}_{ij}^2$ are the squared invariant mass of the (i, j) system, m_π and m_n, m_p are the pion and nucleons masses, respectively. The factor $g_{\pi NN}$ is the pion nucleon coupling constant which is relatively well known [11] ($\frac{g_{\pi NN}^2}{4\pi} = 13.5 - 14.6$). In our calculations the coupling constant is taken as $g_{\pi NN}^2/4\pi = 13.5$.

Using the known strength parameters for the NN and πN scattering fitted to the corresponding total cross sections (the Donnachie-Landshoff model [12]) we obtain $C_{\mathbb{P}}^{NN} = 21.7$ mb, $C_{\mathbb{P}}^{\pi N} = 13.63$ mb, $C_\rho^{\pi N} = 4.23$ mb and assuming Regge factorization [13] $C_{\mathbb{P}}^{\pi\pi} = 8.56$ mb. The pomeron and ρ trajectories determined from elastic and total cross sections are given in the linear approximation ($\alpha_i(t) = \alpha_i(0) + \alpha'_i t$) with $t = k_a^2, \dots, k_i^2$ for pomeron trajectory and $t = t_{1,2}$ for the ρ trajectory

$$\alpha_{\mathbb{P}}(t) = 1.0808 + 0.25t, \quad \alpha_{\mathbb{R}}(t) = 0.5475 + 0.93t, \quad (2.15)$$

where the values of relevant parameters (the intercept $\alpha_i(0)$ and the slope of trajectory α'_i) are also taken from the Donnachie-Landshoff model [12] for consistency. The slope parameter can be written as

$$B(s) = B_0 + 2\alpha'_{\mathbb{P}} \ln\left(\frac{s}{s_0}\right), \quad (2.16)$$

where $s_0 = 1 \text{ GeV}^2$. The value of $B_{\pi\pi}$ is not well known, however the Regge factorization entails $B_{\pi\pi} \approx 2B_{\pi N} - B_{NN}$ [13]. In our calculation we use B_0 : $B_{\pi N} = 6.5 \text{ GeV}^{-2}$, $B_{NN} = 9 \text{ GeV}^{-2}$ and $B_{\pi\pi} = 4 \text{ GeV}^{-2}$. We have parametrized the k_a^2, \dots, k_i^2 dependences in the exponential form (see formulas (2.2) – (2.10)). The parameter $a_\rho = -1.16158$ in order to assure the proper phase of the amplitude (2.11) as dictated by corresponding signature factor.

The extra correction factors $F_{\pi,N}^{off}(k^2)$ (where $k^2 = t_{1,2}, u_{1,2}, s_{ij}$) are due to off-shellness of particles. In the case of our 4-body reaction rather large transferred four-momenta squared k^2 are involved and one has to include non-point-like and off-shellness nature of the particles involved in corresponding vertices. This is incorporated via $F_{\pi NN}(k^2)$ vertex form factors. We parametrize these form factors in the following exponential form:

$$F(t_{1,2}) = \exp\left(\frac{t_{1,2} - m_\pi^2}{\Lambda^2}\right), \quad (2.17)$$

$$F(u_{1,2}) = \exp\left(\frac{u_{1,2} - m_n^2}{\Lambda^2}\right), \quad (2.18)$$

$$F(s_{ij}) = \exp\left(\frac{-(s_{ij} - m_p^2)}{\Lambda^2}\right). \quad (2.19)$$

² In the following for brevity we shall use notation $t_{1,2}$ which means t_1 or t_2 .

While four-momenta squared of transferred pions $t_{1,2} < 0$, it is not the case for transferred neutrons where $u_{1,2} < m_n^2$. In general, the cut-off parameter Λ_{off} is not known but in principle could be fitted to the (normalized) experimental data. From our general experience in hadronic physics we expect $\Lambda_{off} \sim 1$ GeV. Typical values of the πNN form factor parameters used in the meson exchange models are $\Lambda = 1.2\text{--}1.4$ GeV [14], however the Gottfried Sum Rule violation prefers smaller $\Lambda \approx 0.8$ GeV [15]. In our calculation, if not otherwise mentioned, we use $\Lambda = \Lambda_{off} = 1$ GeV. We shall discuss how uncertainties of the form factors influence our final results.

The diagram j) is topologically identical to the dominant diagram for the $pp \rightarrow pp\pi^+\pi^-$ process [10]. There, however, the pomeron-pomeron, pomeron-reggeon and reggeon-pomeron exchanges are the dominant processes.

The ρ -meson/reggeon exchange is known to have not only spin-conserving part (see formula (2.2)) but also quite sizeable spin-flip components. Therefore for this specific process we have to include also the spin-flip components. We write the single spin-flip (SSF) and double spin-flip (DSF) amplitudes as:

$$\begin{aligned} \mathcal{M}_{\lambda_a \lambda_b \rightarrow \lambda_1 \lambda_2}^{(SSF)} &= \sqrt{2} \delta_{\lambda_a, \lambda_1 = -\lambda_a} \frac{\sqrt{-t_1}}{2m_N} r_T (a_\rho - i) s_{13} C_\rho^{\pi N} \left(\frac{s_{13}}{s_0} \right)^{\alpha_\rho(t_1)-1} \exp \left(\frac{B_{\pi N}}{2} t_1 \right) \\ &\times F_\pi^{off}(k_\pi^2) \frac{1}{k_\pi^2 - m_\pi^2} F_\pi^{off}(k_\pi^2) \\ &\times \sqrt{2} \delta_{\lambda_b, \lambda_2} (a_\rho - i) s_{24} C_\rho^{\pi N} \left(\frac{s_{24}}{s_0} \right)^{\alpha_\rho(t_2)-1} \exp \left(\frac{B_{\pi N}}{2} t_2 \right) \\ &+ \text{crossed term} , \end{aligned} \quad (2.20)$$

$$\begin{aligned} \mathcal{M}_{\lambda_a \lambda_b \rightarrow \lambda_1 \lambda_2}^{(SSF)} &= \sqrt{2} \delta_{\lambda_a, \lambda_1} (a_\rho - i) s_{13} C_\rho^{\pi N} \left(\frac{s_{13}}{s_0} \right)^{\alpha_\rho(t_1)-1} \exp \left(\frac{B_{\pi N}}{2} t_1 \right) \\ &\times F_\pi^{off}(k_\pi^2) \frac{1}{k_\pi^2 - m_\pi^2} F_\pi^{off}(k_\pi^2) \\ &\times \sqrt{2} \delta_{\lambda_b, \lambda_2 = -\lambda_b} \frac{\sqrt{-t_2}}{2m_N} r_T (a_\rho - i) s_{24} C_\rho^{\pi N} \left(\frac{s_{24}}{s_0} \right)^{\alpha_\rho(t_2)-1} \exp \left(\frac{B_{\pi N}}{2} t_2 \right) \\ &+ \text{crossed term} , \end{aligned} \quad (2.21)$$

$$\begin{aligned} \mathcal{M}_{\lambda_a \lambda_b \rightarrow \lambda_1 \lambda_2}^{(DSF)} &= \sqrt{2} \delta_{\lambda_a, \lambda_1 = -\lambda_a} \frac{\sqrt{-t_1}}{2m_N} r_T (a_\rho - i) s_{13} C_\rho^{\pi N} \left(\frac{s_{13}}{s_0} \right)^{\alpha_\rho(t_1)-1} \exp \left(\frac{B_{\pi N}}{2} t_1 \right) \\ &\times F_\pi^{off}(k_\pi^2) \frac{1}{k_\pi^2 - m_\pi^2} F_\pi^{off}(k_\pi^2) \\ &\times \sqrt{2} \delta_{\lambda_b, \lambda_2 = -\lambda_b} \frac{\sqrt{-t_2}}{2m_N} r_T (a_\rho - i) s_{24} C_\rho^{\pi N} \left(\frac{s_{24}}{s_0} \right)^{\alpha_\rho(t_2)-1} \exp \left(\frac{B_{\pi N}}{2} t_2 \right) \\ &+ \text{crossed term} . \end{aligned} \quad (2.22)$$

Here we have introduced one more phenomenological (dimensionless) parameter r_T . It is known to be of $3 < r_T < 8$ [16] (see also [17]). In the present calculations we take $r_T = 7.5$ [16]. The above components do not interfere with the spin-conserving ones and can be calculated separately.

The parameterization of amplitude with $\rho\rho$ reggeon exchanges (diagram j) can not be used in the region of resonances in πN subsystems (see [10]). Therefore, the amplitude used

in the calculations must contain restrictions on the four-body phase space. To exclude the regions of resonances we improve the parameterization of the amplitudes (2.11, 2.20, 2.21 and 2.22) by multiplying by a purely phenomenological smooth cut-off correcton factor:

$$f_{cont}^{\pi N}(W_{ik}) = \frac{\exp\left(\frac{W-W_0}{a}\right)}{1 + \exp\left(\frac{W-W_0}{a}\right)}. \quad (2.23)$$

The parameter W_0 gives the position of the cut and parameter a describes how sharp is the cut off. For large energies $f_{cont}^{\pi N}(W_{ik}) \approx 1$ and close to kinematical threshold $f_{cont}^{\pi N}(W_{ik}) \approx 0$. In our calculation we take $W_0 = 2$ GeV and $a = 0.2$ GeV.

The cross section is obtained by assuming a general $2 \rightarrow 4$ reaction:

$$\sigma = \int \frac{1}{2s} |\overline{\mathcal{M}}|^2 (2\pi)^4 \delta^4(p_a + p_b - p_1 - p_2 - p_3 - p_4) \frac{d^3 p_1}{(2\pi)^3 2E_1} \frac{d^3 p_2}{(2\pi)^3 2E_2} \frac{d^3 p_3}{(2\pi)^3 2E_3} \frac{d^3 p_4}{(2\pi)^3 2E_4}. \quad (2.24)$$

To calculate the total cross section one has to calculate 8-dimensional integral numerically. The details how to conveniently reduce the number of kinematical integration variables are given elsewhere [10].

B. Absorptive corrections

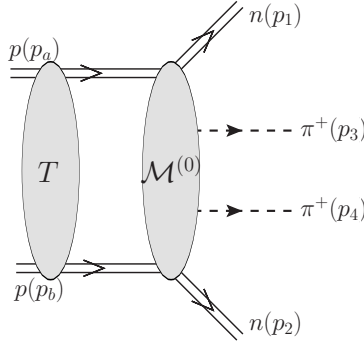


FIG. 2: Schematic diagram for absorption effects due to proton-proton interaction.

The absorptive correction in Fig.2 are calculated as described in [6] for the three body processes. Here the absorptive correction to the bare amplitude (see Fig.1) can be written as:

$$\delta \mathcal{M}_{\lambda_a \lambda_b \rightarrow \lambda_1 \lambda_2} = \int \frac{d^2 k_t}{2(2\pi^2)} T(s, \vec{k}_t) \mathcal{M}_{\lambda_a \lambda_b \rightarrow \lambda_1 \lambda_2}^{(0)}. \quad (2.25)$$

Above $\mathcal{M}_{\lambda_a \lambda_b \rightarrow \lambda_1 \lambda_2}^{(0)}$ is a bare amplitude calculated as described in the previous subsection. $T(s, \vec{k}_t)$ is an elastic proton-proton amplitude for the appropriate energy. It can be conveniently parametrized as:

$$T(s, \vec{k}_t) = i\sigma_{tot}^{pp}(s) \exp(-B_{NN} k_t^2 / 2). \quad (2.26)$$

Again the Donnachie-Landshoff parametrization [12] of the total pp or $p\bar{p}$ cross sections can be used to calculate the absorption effects.

Absorption effects for exclusive Higgs production are discussed e.g. in Ref.[18].

TABLE I: Full-phase-space integrated cross section (in mb) for exclusive $nn\pi^+\pi^+$ production at selected center-of-mass energies and different values of the form factor parameters. In parantheses we show cross sections including absorption effects.

	W = 0.2 TeV	W = 0.9 TeV	W = 2.36 TeV	W = 7 TeV
$\Lambda = 0.8 \text{ GeV}, \Lambda_{off} = 1 \text{ GeV}$	0.4	0.53	0.66	0.84
$\Lambda = \Lambda_{off} = 1 \text{ GeV}$	1.11 (0.51)	1.48 (0.58)	1.84 (0.63)	2.34 (0.68)
$\Lambda = 1.2 \text{ GeV}, \Lambda_{off} = 1 \text{ GeV}$	2.09	2.79	3.49	4.45

III. RESULTS

We shall show our predictions for the $pp \rightarrow nn\pi^+\pi^+$ reaction for several differential distributions in different variables at selected center-of-mass energies $W = 0.2, 0.5, 0.9, 2.36, 7 \text{ TeV}$. The cross section slowly rises with incident energy. In general, the higher energy the higher absorption effects. The results depend on the value of the nonperturbative, a priori unknown parameter of the form factor responsible for off-shell effects. In Table I we have collected integrated cross sections for selected energies and different values of the model parameters. We show how the uncertainties of the form factor parameters affect our final results.

In Fig.3 we show distributions in pseudorapidity ($\eta = -\ln(\tan \frac{\theta}{2})$, where θ is the angle between the particle momentum and the beam axis) for the $pp \rightarrow nn\pi^+\pi^+$ reaction. The discussed reaction is very unique because not only neutrons but also pions are produced in very forward or very background directions forming a gigantic gap in pseudorapidity between the produced pions, about 12 units at $W = 7 \text{ TeV}$. While neutrons can be measured by the ZDC's the measurement of very forward/backward pions requires further studies. A possible evidence of the reaction discussed here is a signal from both ZDC's and no signal in the central detector.

In Fig.4 we present rapidity distributions of pions y_{π^+} and rapidity distributions of neutrons y_n . Please note a very limited range of rapidities shown in the figure. The contributions for individual diagrams a) – i) (see Fig.1) are also shown. The diagram d) gives the largest contribution. One can observe specific symmetries between different contributions on the left and right panels. For instance the long-dash-dotted line on the left panel (corresponding to diagram b)) is symmetric to the dashed line on the right panel (corresponding to diagram c)). Clearly, a significant interference effect can be seen.

For completeness in Fig.5 we show the contribution of the diagram j) with double reggeon exchange ($\rho\rho$) which could not be seen in the previous plot (the dashed line does not include correction factor (2.23)). The difference between the solid and dashed lines shows the rapidity regions where the nucleon resonances may contribute. The latter contributions are rather difficult to calculate. In contrast to the other mechanisms it extends over broader range of rapidities. For the LHC energy $\sqrt{s} = 7 \text{ TeV}$ it is, however, very small (see right panel). We have also done similar calculations for the RHIC energy $\sqrt{s} = 500 \text{ GeV}$ (see left panel). The cross section corresponding to this mechanism increased by more than two orders of magnitude compared to $\sqrt{s} = 7 \text{ TeV}$, but is still negligible compared to the other contributions.

Can the much smaller $\rho\rho$ contribution be identified experimentally? In Fig.6 we show two-

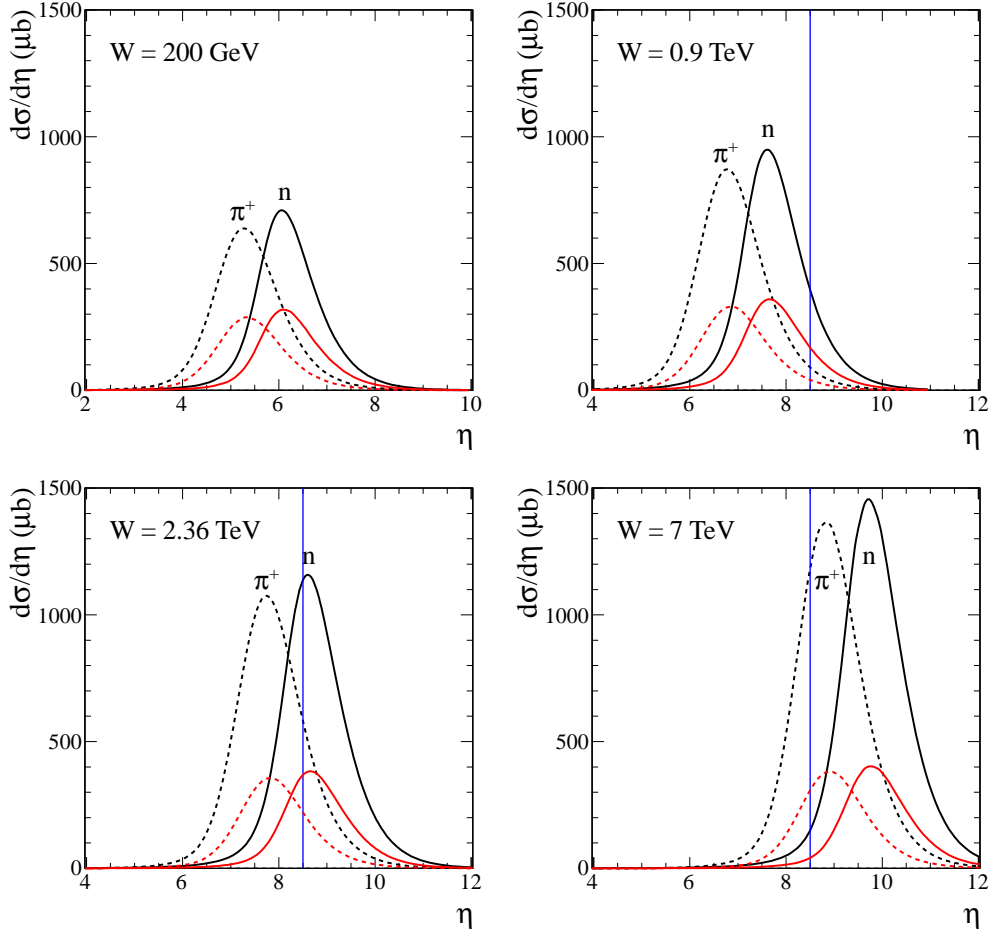


FIG. 3: Differential cross section $d\sigma/d\eta$ for neutrons (solid lines) and pions (dotted lines) at the center-of-mass energies $W = 0.2, 0.9, 2.36, 7 \text{ TeV}$. The smaller bumps include absorption effects calculated in a way described in subsection II B. In this calculation we have used $\Lambda = \Lambda_{off} = 1 \text{ GeV}$. The vertical lines at $\eta = \pm 8.5$ are the lower limits of the CMS ZDC's. The details about RHIC ZDC's can be found in Ref.[19].

dimensional distribution in (y_3, y_4) space. The $\rho\rho$ component is placed along the diagonal $y_3 = y_4$ while the other contributions some distance from the diagonal. Therefore imposing 2-dim cuts in the (y_3, y_4) space one could separate the small $\rho\rho$ contribution. A very good one-dimensional observable which can be used for the separation of the process under discussion could be differential cross section $d\sigma/dy_{diff}$, where $y_{diff} = y_3 - y_4$ and experimentally charged pions should be taken at random (see Fig.7, $y_{\pi, first} = y_3$ or y_4 and $y_{\pi, second} = y_4$ or y_3).

One can see that the double reggeon exchange mechanism populates midrapidities of the pions and therefore can be measured either at RHIC or at LHC. In Table II we have collected cross section for this component separately for double spin conserving (DSC), single spin flip (SSF) and double spin flip (DSF) contributions. All this spin contributions are of similar size. The total contribution is about half of nb at RHIC (500 GeV) and a few pb at LHC (7 TeV).

In Fig.8 we show distribution of neutrons and pions in the Feynman variable $x_F = 2p_{||}/\sqrt{s}$. In this observable the neutrons and pions are well separated. The position of peaks is almost

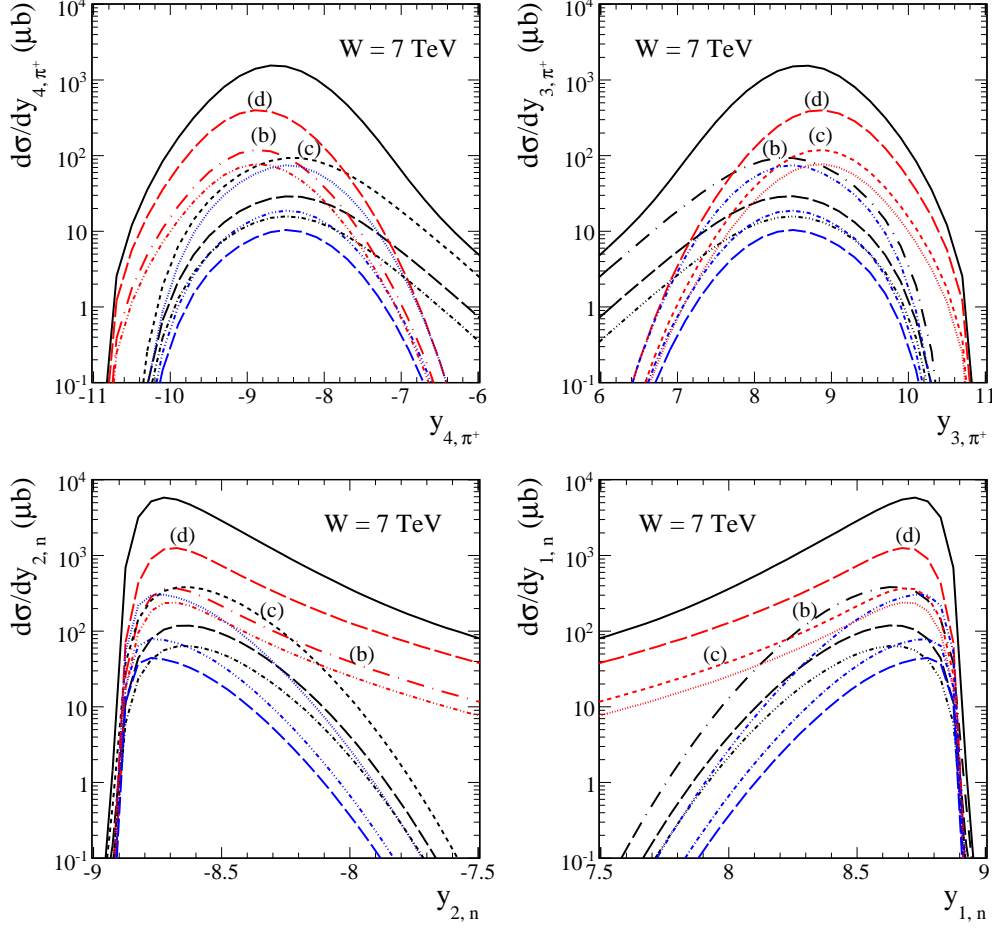


FIG. 4: Differential cross sections $d\sigma/dy_{\pi^+}$ and $d\sigma/dy_n$ at $W = 7$ TeV. The bold solid line represent the coherent sum of all amplitudes. The long-dashed (black), long-dash-dotted, dashed, long-dashed (red online), dash-dot-dot-dotted, dotted, dash-dotted, dash-dot-dotted, long-dashed (blue online) lines correspond to contributions from a) – i) diagrams. The red, black and blue lines correspond to diagrams when neutron, pion and proton are off-mass-shell, respectively.

independent of energy. While pions are produce at relatively small x_F the neutrons carry large fractions of the parent protons. The situation is qualitatively the same for all energies.

The distribution in pion-pion invariant mass is shown in Fig.9. Unique for this reaction, very large two-pion invariant masses are produced (see e.g. Ref.[10]). The larger energy the larger two-pion invariant masses (left panel). We show also distributions with different values of the form factor parameter in order to demonstrate the cross section uncertainties (right panel). The absorption effects almost uniformly reduce the cross section.

The distributions in the transverse momentum of neutrons and pions are shown in Fig.10. The figure shows that the typical transverse momenta are rather small but large enough to be measured. The distributions for neutrons are rather similar to those for pions.

The energy distributions of neutrons are presented in Fig.11. Generally the larger collision energy the larger energy of outgoing neutrons. When combined with the previous plot it becomes clear that the neutrons are produced at very small polar angles (large pseudora-

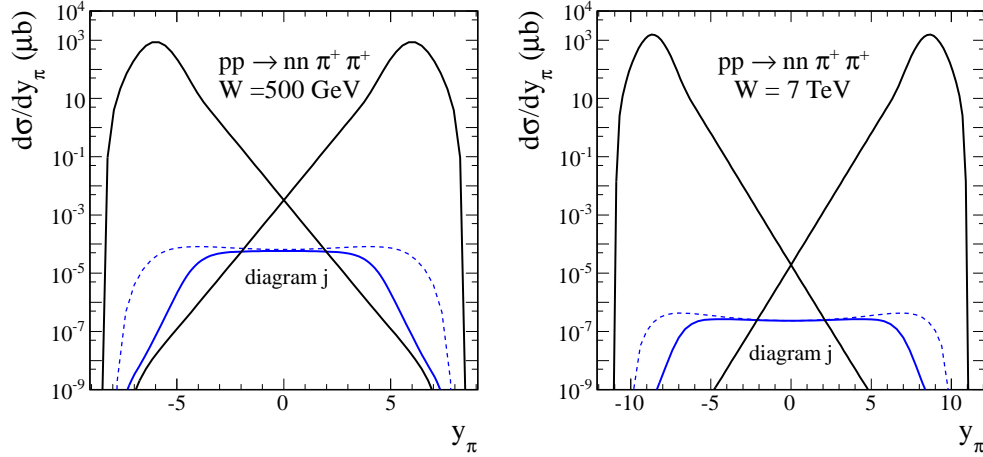


FIG. 5: Differential cross sections $d\sigma/dy_{\pi^+}$ at $W = 500$ GeV (left) and $W = 7$ TeV (right). The lines represent the coherent sum of all amplitudes from a) – i) diagrams and the contribution of diagram j) with $\rho\rho$ reggeon exchanges. The dashed line does not include correction factor (2.23).

TABLE II: Full-phase-space integrated cross section (in nb) for exclusive $\pi^+\pi^+$ production for the amplitude with the $\rho\rho$ reggeon exchanges (diagram j) in Fig.1) at the center-of-mass energies $W = 0.5, 7$ TeV. The meaning of the acronyms: DCS - double spin conserving, SSF - single spin flip, DSF - double spin flip.

	$W = 0.5$ TeV	$W = 7$ TeV
DSC	0.1	9.81(-4)
SSF	0.11	8.3(-4)
DSF	0.11	6.34(-4)
full	0.43	3.28(-3)

pidities) and can be measured by the ZDC's (see also Fig.3).

In Fig.12 we show two-dimensional correlations between energies of both neutrons measured in both ZDC's. The figure shows that the energies of both neutrons are almost not correlated i.e. the shape (not the normalization) of $d\sigma/dE_{n_1}$ ($d\sigma/dE_{n_2}$) is almost independent of E_{n_2} (E_{n_1}). There should be no problem in measuring energy spectra of neutrons on both sides as well as two-dimensional correlations in (E_{n_1}, E_{n_2}) .

Finally in Fig.13 we present the distributions in azimuthal angle between outgoing neutrons. Clearly a preference of back-to-back emissions can be seen. The measurement of azimuthal correlations of neutrons will be not easy with first version of ZDC's as only horizontal position can be measured. Still correlations of horizontal hit positions on both sides could be interesting. A new correlation observable, taking into account possibilities of the apparatus, should be proposed. In contrast the two π^+ 's are almost not correlated in azimuthal angle. Such a distribution may be not easy to measure.

We have shown that at present the reaction under consideration can be strictly measured only in a rather limited part of the phase space (midrapidities of pions) where the cross section is rather small and where the double reggeon $\rho\rho$ mechanism dominates. In Table

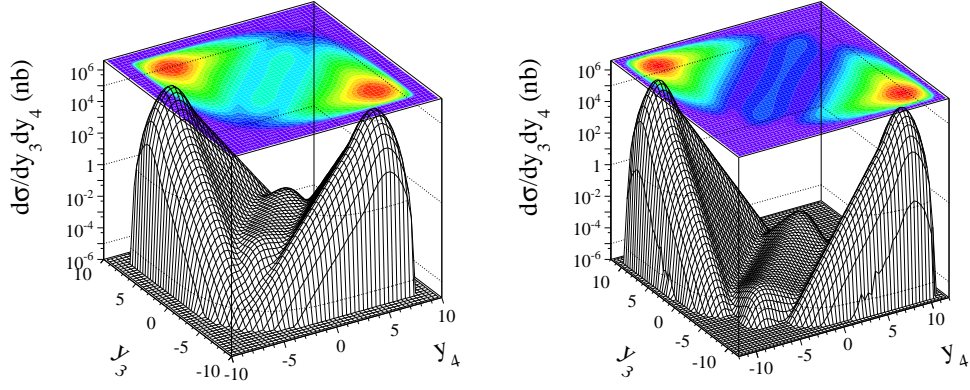


FIG. 6: Differential cross sections in (y_3, y_4) space at $W = 500$ GeV (left) and $W = 7$ TeV (right). The coherent sum of all amplitudes for diagrams a) – i) and the contribution of diagram j) with $\rho\rho$ reggeon exchanges placed along the diagonal are presented.

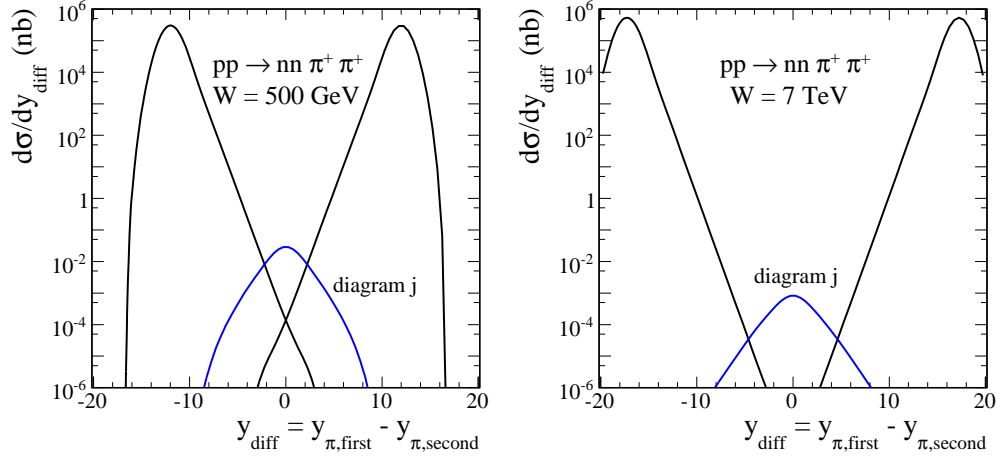


FIG. 7: Differential cross sections $d\sigma/dy_{diff}$ at $W = 500$ GeV (left) and $W = 7$ TeV (right). The lines represent the coherent sum of all amplitudes from a) – i) diagrams and the contribution of diagram j) with $\rho\rho$ reggeon exchanges. No absorption effects were included here.

III we have collected the cross sections in nb for different experiments at LHC and RHIC. At LHC where the separation of the double-reggeon exchange mechanism is possible the cross section is rather small of the order of a fraction of pb. At RHIC the cross section with experimental cuts should be easily measurable as it is of the order of a fraction of nb.

IV. CONCLUSIONS

We have estimated cross sections and calculated several differential observables for the exclusive $pp \rightarrow nn\pi^+\pi^+$ reaction. The full amplitude was parametrized in terms of leading pomeron and subleading reggeon trajectories. The latter turned out to be of the order of 1 % i.e. practically negligible. There is a diagram when pomeron exchange is not possible

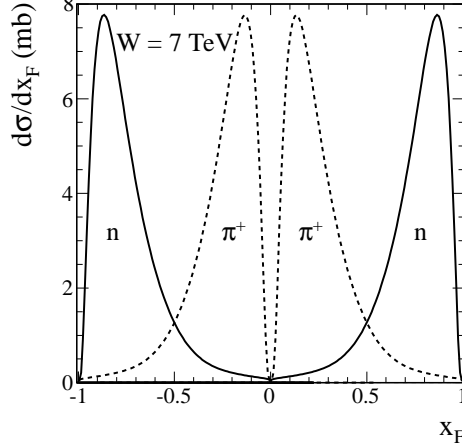


FIG. 8: Differential cross section $d\sigma/dx_F$ for the $pp \rightarrow nn\pi^+\pi^+$ reaction at $W = 7$ TeV. No absorption effects were included here.

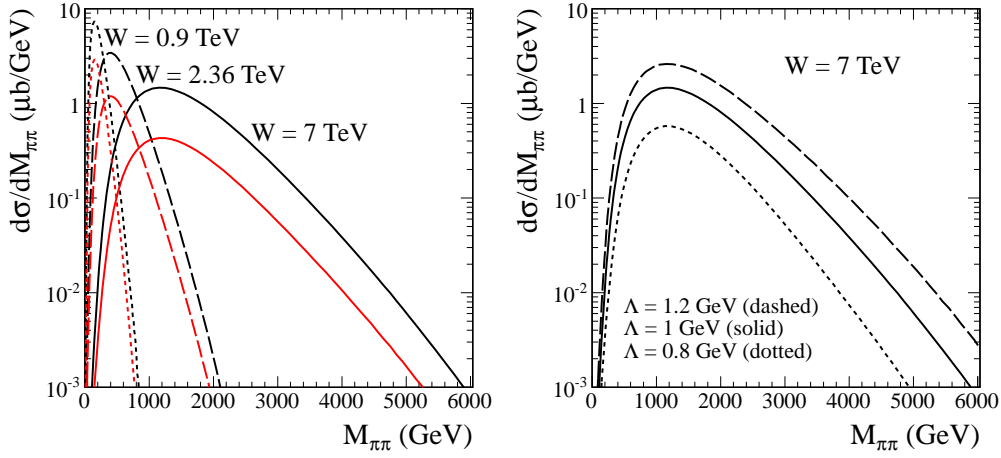


FIG. 9: Differential cross section $d\sigma/dM_{\pi\pi}$ for the $pp \rightarrow nn\pi^+\pi^+$ reaction at $W = 0.9, 2.36, 7$ TeV (left panel). The lower curves correspond to calculations with absorption effects. Right panel shows cross section obtained with different values of the form factor parameter $\Lambda = 0.8$ GeV (dotted line), $\Lambda = 1$ GeV (solid line) and $\Lambda = 1.2$ GeV (dashed line). No absorption effects are included here.

and charge exchange of the ρ reggeon is the only possibility. Also the contribution of this diagram with the cross section concentrated at midrapidities is very small. The situation changes at smaller energies. The $\rho\rho$ exchange process although with small cross section at LHC can be separated out in the two-dimensional space of rapidities of both pions.

Large cross sections have been obtained, bigger than for the $pp \rightarrow pp\pi^+\pi^-$ reaction [10]. Several mechanisms contribute to the cross section, which leads to an enhancement of the cross section due to interference effects.

The specificity of the reaction is that both neutrons and pions are emitted in very forward/backward directions, producing a huge rapidity gap at midrapidities. While the neutrons could be measured by the ZDC's, the identification of pions may be difficult. We

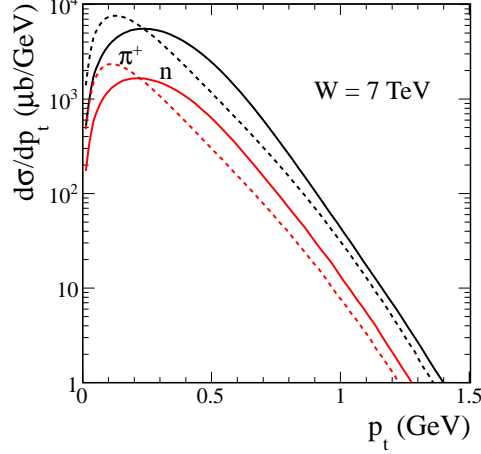


FIG. 10: Differential cross section $d\sigma/dp_t$ for the $pp \rightarrow nn\pi^+\pi^+$ reaction at $W = 7$ TeV. The solid and dotted lines correspond to the distribution in the transverse momentum of neutrons and pions, respectively. The lower curves correspond to calculations with absorption effects.

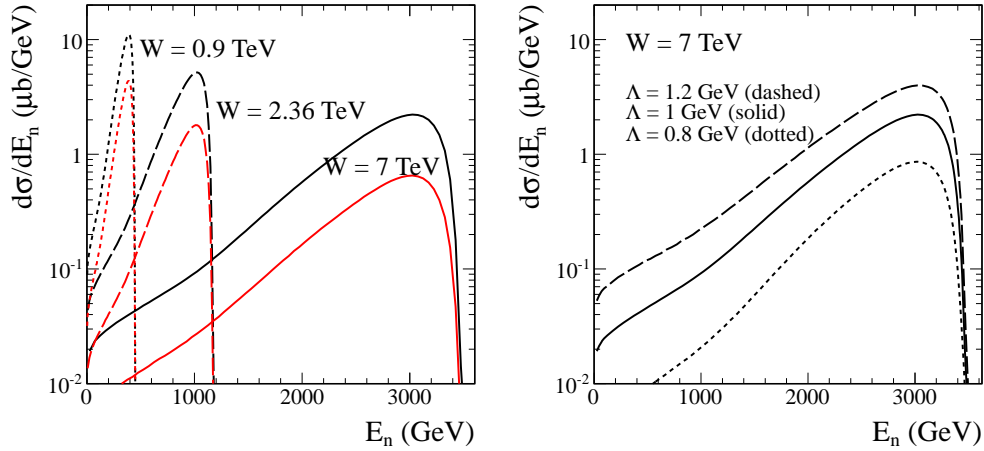


FIG. 11: Differential cross section $d\sigma/dE_n$ for the $pp \rightarrow nn\pi^+\pi^+$ reaction at $W = 0.9, 2.36, 7$ TeV (left panel). The lower curves correspond to calculations with absorption effects. Right panel shows cross section obtained with different values of the form factor parameter $\Lambda = 0.8$ GeV (dotted line), $\Lambda = 1$ GeV (solid line) and $\Lambda = 1.2$ GeV (dashed line).

think that the measurement of both neutrons and observation of large rapidity gap is a very good signature of the considered reaction. We expect the cross section for the $nn\pi^+\pi^+\pi^0$, $nn\pi^+\pi^+\pi^0\pi^0$, etc. to be much smaller. In addition for events with larger number of pions the rapidity gap would be destroyed. Therefore the formally kinematically incomplete measurement of two neutrons only could be relatively precise. We have found that the neutrons measured in ZDC's seem to be almost uncorrelated in energies.

We have made predictions for azimuthal angle correlations of outgoing neutrons. Such distribution should be possible to measure in a future. At present at CMS only horizontal position can be measured. We have predicted back-to-back correlations with a sizeable diffusion.

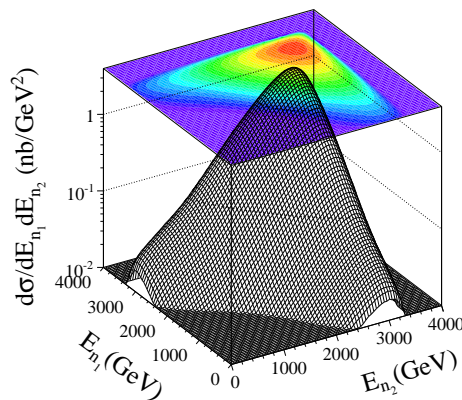


FIG. 12: Differential cross section $d\sigma/dE_{n_1}dE_{n_2}$ for the $pp \rightarrow nn\pi^+\pi^+$ reaction at $W = 7$ TeV.

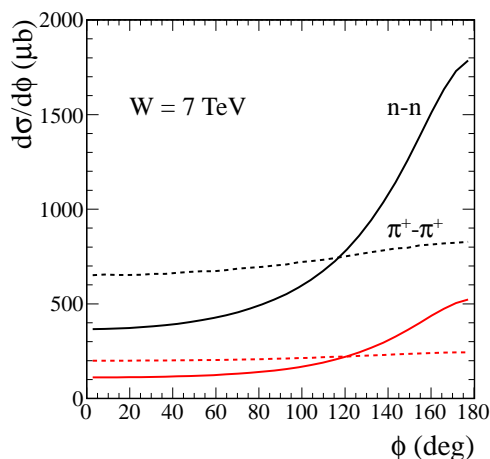


FIG. 13: Azimuthal angle correlations between neutrons and beetwen pions for the $pp \rightarrow nn\pi^+\pi^+$ reaction at $W = 7$ TeV. The lower curves correspond to calculations with absorption effects included.

We have included elastic rescattering effects in a way used recently for the three body processes. These effects lead to a substantial damping of the cross section. The bigger energy the larger the effect of damping. Other processes (e.g. inelastic intermediate states) could lead to additional damping. At present there is no full understanding of the absorption effects.

Future measurements, if possible, should be very useful in shedding new light on absorption effects which are essential for understanding exclusive processes, even such important ones as exclusive production of the Higgs boson.

There is an attempt to install forward shower counters in the LHC tunnel. Most probably they will not be able to measure energy of the pions but they can signal some activity there. From the theory side "some activity" will mean, with a high probability, just one π^+ on one side and the other π^+ on the other side.

TABLE III: Cross section (no absorption effects) with different experimental cuts on $p_{t,\pi}$, η_π and η_n .

	W (TeV)	$p_{t,\pi}$	$ \eta_\pi >$	$ \eta_n _{ZDC} >$	$\sigma_{\rho\rho}$ (nb)	σ_{other} (nb)
ALICE	7	0.15	0.9	8.7	8.45(-5)	4.2(-9)
ALICE	7	0.15	1.2	8.7	1.45(-4)	1.34(-8)
ATLAS	7	0.5	2.5	8.3	2.91(-5)	1.62(-6)
CMS	7	0.75	2.4	8.5	2.46(-6)	5.04(-7)
RHIC	0.5	0.2	1	—	1.98(-2)	2.3(-4)

Acknowledgments

We are indebted to Michael Murray for an interesting discussion on a possibility of a measurement of the discussed reaction and Wolfgang Schäfer for a discussion of the reaction mechanisms. This study was partially supported by the Polish grant of MNiSW No. N202 249235.

-
- [1] M.G. Albrow *et al.* [FP420 Collaboration], arXiv:0806.0302 [hep-ex], published in J. Inst.: <http://www.iop.org/EJ/abstract/1748-0221/4/10/T10001>.
 - [2] O.A. Grachov *et al.* [CMS Collaboration], J. Phys. Conf. Ser. **160** (2009) 012059.
 - [3] M. Murray, a talk at "Diffractive and Electromagnetic processes at the LHC", Trento, January 4-8, 2010.
 - [4] J. Peter *et al.* [ATLAS Collaboration], CERN-LHCC-2007-001, LHCC-I-016, <http://cdsweb.cern.ch/record/1009649>.
 - [5] V.A. Petrov, R.A. Ryutin and A.E. Sobol, Eur. Phys. J. **C65** (2010) 637; A.E. Sobol, R.A. Ryutin, V.A. Petrov and M. Murray, arXiv:1005.2984 [hep-ph].
 - [6] W. Schäfer and A. Szczurek, Phys. Rev. **D76** (2007) 094023.
 - [7] Z. Ouyang, J. J. Xie, B. S. Zou, H. S. Xu, Int.J.Mod.Phys. **E18** (2009) 281; Xu Cao, Bing-Song Zou, H. S. Xu, arXiv:nucl-th/1004.0140.
 - [8] A. Szczurek and P. Lebiedowicz, Nucl. Phys. **A826** (2009) 101.
 - [9] P. Lebiedowicz, A. Szczurek and R. Kamiński, Phys. Lett. **B680** (2009) 459.
 - [10] P. Lebiedowicz and A. Szczurek, Phys. Rev. **D81** (2010) 036003.
 - [11] T.E.O. Ericson, B. Loiseau and A.W. Thomas, Phys. Rev. **C66** (2002) 014005.
 - [12] A. Donnachie and P.V. Landshoff, Phys. Lett. **B296** (1992) 227.
 - [13] A. Szczurek, N.N. Nikolaev and J. Speth, Phys. Rev. **C66** (2002) 055206.
 - [14] R. Machleidt, K. Holinde and Ch. Elster, Phys. Rep. **149** (1987) 1; D.V. Bugg, R. Machleidt, Phys. Rev. **C52** (1995) 1203.
 - [15] A. Szczurek and J. Speth, Nucl. Phys. **A555** (1993) 249; B.C. Pearce, J. Speth and A. Szczurek, Phys. Rep. **242** (1994) 193; J. Speth and A.W. Thomas, Adv. Nucl. Phys. **24** (1997) 83.
 - [16] G.L. Kane and A. Seidl, Rev. Mod. Phys. **48** (1976) 309.
 - [17] A.C. Irving and R.P. Worden, Phys. Rep. **C34** (1977) 117.

- [18] V.A. Khoze, A.D. Martin and M.G. Ryskin, Eur. Phys. J. **C18** (2000) 167;
U. Maor, AIP Conf. Proc. **1105** (2009) 248.
- [19] C. Adler, A. Denisov, E. Garcia, M. Murray, H. Stroebele and S. White, Nucl. Instrum. Meth. **A470** (2001) 488.